MATERIALS AND METHODS

Chemicals

A high-density polyethylene (PE) film with no additives was kindly supplied by Mitsui Chemical Industries, Ltd. (Tokyo, Japan). Its thickness was 0.35 mm and the weight-average molecular weight was 153,000. We used acrylic acid monomer obtained from Nakalai Tesque Inc. (Kyoto, Japan) after conventional distillation. Bovine serum albumin (BSA) and Type-I collagen from porcine tendon (cell-matrix, type I-P) were purchased from Sigma Chemical Co. (St. Louis, MO) and Nitta Gelatin Co., Ltd. (Osaka, Japan), respectively. Arg-Gly-Asp-Ser (RGDS) peptide was kindly donated by Yoshiaki Hirano (Osaka Institute of Technology, Japan). Hanks's balanced salt solution (HBSS) and Ham's F12 medium were purchased from Life Technologies, Inc. (Grand Island, NY). We purchased and used without further purification 1-ethyl-3-(3-dimethyl aminopropyl)-carbodiimide (WSC) and other chemicals from Wako Pure Chemical Industries (Osaka, Japan).

Immobilization of proteins onto PE film

Protein immobilization onto the surface of PE film was carried out according to the method reported previously.[1] Briefly, we subjected PE film to corona discharge to introduce peroxides onto the surface and then placed it in a solution containing acrylic acid monomer in a Pyrex tube, followed by degassing procedure. The tube was kept at 60°C for 1 h to allow the graft polymerization of the monomer to proceed onto the PE surface. After placing grafted film in 0.1 *M* acetic acid solution (pH 4.5), we added WSC to the solution. The film was transferred to a protein solution to immobilize the protein onto the grafted film. The amount of protein immobilized onto the film was estimated by the ninhydrin method after hydrolysis of immobilized protein. The immobilized films were sterilized by immersion in 70% ethanol solution for 12 h at 4°C, and subsequently placed in sterile phosphate-buffered saline solution (PBS, pH 7.4) to remove ethanol just before the assay described below.

Cell differentiation assay by micromass culture of midbrain cells

MB micromass culture was performed according to the method previously reported.[2] Figure 1 shows the scheme of the assay of the MB micromass culture system. Briefly, MB tissues were separated from the embryos of pregnant Wister rats (Japan SLC Inc., Shizuoka, Japan) on day 13 of gestation. MB tissues were dissociated into individual cells by successive washing in calcium- and magnesium-free HBSS, and by trypsin digestion for 10 min at 37°C. The cells were suspended at a density of 5×10^6 cells per mL in culture medium consisting of Ham's F12 with 10% fetal calf serum (F12–10% FCS). Aliquots of 20 μL of cell suspension were seeded on PE film or protein-immobilized PE film placed into 12-well cell culture plates, followed by the addition of 1 mL of F12–10% FCS after 2 h and an incubation at 37°C in a 5% CO_2–95% air atmosphere for 1 wk. After the cells were fixed and stained with hematoxylin, the extent of nerve cell differentiation was assessed by counting the differentiated foci under a dissecting microscope. The differentiated cells on each test film were photographed with a digital microscope VH-8000 (Keyence Co., Ltd., Osaka, Japan). Cytotoxicity of the films was estimated by the alamar Blue™ assay (BioSource International, Inc., Camarillo, CA), which incorporates an oxidation-reduction indicator based on detection of metabolic activity.[4] After 1 wk of incubation, aliquots of 50 μL alamar Blue solution were added to each test dish, followed by a further 4-hr incubation. The fluorescence intensity (excitation 530 nm, emission 570 nm) of supernatant was estimated by CytoFluor™ II (PerSeptive Biosystems,

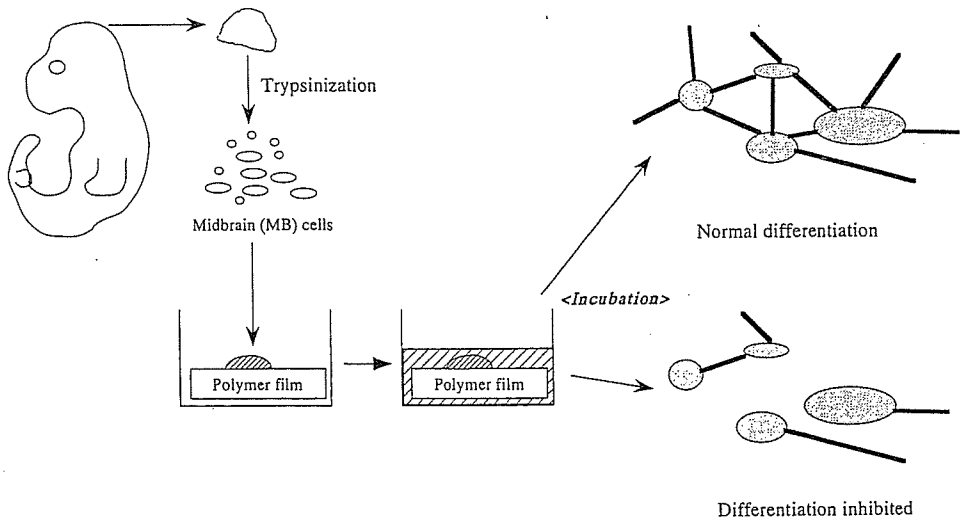

Figure 1. Schematic illustration of micromass culture system using MB cells.

Flamingham, MA). The effects of condition media of MB tissues cultured on Various PE films were estimated as follows: MB cells were collected and cultured on PE films as above, followed by incubation at 37°C in a 5% CO_2–95% air atmosphere. Then, supernatants of MB cell culture (condition media) were collected after 3 days, followed by the addition of 1 mL F12–10% FCS and an additional 4-day incubation. The condition media were collected again after cultivation of MB cells. All condition media collected were kept at −80°C until we detected an effect on differentiation and proliferation of MB cells. To detect the effect of condition medium, MB cells were subjected to the micromass culture on a normal culture dish, followed by the addition of 500 μL F12–10% FCS and 500 μL the condition medium. The effect was estimated as described above after 1-wk incubation. The experiments were repeated at least three times.

Effects of condition medium from MB cell culture on PC12 differentiation

To examine effects of the condition medium on neuronal cell differentiation, we cultured PC12 cells as model neuronal cells, using the condition mediums from MB cultured on various kinds of PE films. PC12 cells were kindly donated by Shuichi Koizumi (National Institute of Health Sciences, Tokyo, Japan) and cultured in a medium consisting of Dulbecco's modified Eagle's medium (MEM) supplemented with 5% FCS and 5% heat-inactivated horse serum. The cells were suspended in the medium at the density of 2×10^4 per mL. An aliquot of 500 μL of the suspension was added to 24-well collagen-coated culture plates, followed by a 5-h incubation to adhere the cells onto the plates. Then, an aliquot of 100 μL of the condition medium was added to each plate, and axonal growth from the cells was observed daily by light microscopy to estimate a differentiation level of PC12. For positive control of differentiation of the cell, 25 μg of nerve growth factor (NGF; purchased from Wako Pure Chemical Ltd., Osaka, Japan) was added to the plates and treated as above.

Statistic analysis

All data were expressed as the mean value ± standard deviation of the data obtained from each experiment and treated statistically with Student's *t* test.

RESULTS

Figure 2 shows foci of MB cells cultured on various protein-immobilized PE films after a 7-day incubation. MB cells formed many foci, and many neuron-like fibers were observed between the foci when cultured on polystyrene and collagen-coated culture dishes. The MB cells on untreated PE films developed few neuron fibers compared to those on the polystyrene culture dish, and the cells did not gather to create cell foci. However, a protein immobilization onto PE caused neuron fibers to connect between foci, although the number of fibers observed was affected by the kind of protein immobilized. In Figure 2, it is clear that the size of the focus was also affected by the protein immobilized. When collagen was immobilized, the observed foci were smaller than the other foci. However, the number of fibers from each focus was greater than that of the other PE film, indicating differentiation of MB cells promoted by collagen. Table I indicates the number of differentiated foci of MB cells on various PE films. The PE film inhibited differentiation of MB cells, as seen in the small number of differentiated foci. In addition, the PE film showed high cytotoxicity compared with a control dish. This may be one reason why the differentiation of MB cells was inhibited. By protein immobilization, however, the number of differentiated foci increased in comparison with those of the PE film. Moreover, collagen and RGDS peptide immobilization increased the number of the foci more than that observed on the culture dish.

We estimated the effects of condition media on MB cell differentiation to see whether they include some factors affecting cell differentiation. Table II shows the effects of condition media on MB cell differentiation on a collagen-coated culture dish. Addition of the condition medium from MB cell cultivation on all kinds of PE films showed a cytotoxic effect on MB cells. In addition, the cytotoxic effect was enhanced when collected after 7 days of incubation. This effect might be ascribed to a loss of nutrition from the medium during the first cell culture. The differentiation of MB cells on a collagen-coated dish was suppressed by the addition of the media from MB cells on various PE films on day 3. However, a condition medium from MB cell on collagen-immobilized PE film on day 7 showed many differentiated foci, as many as were induced by a condition medium from MB cells on a collagen-coated culture dish on day 7. Although the medium from the collagen-immobilized film revealed an enhanced effect on differentiation, addition of the condition media from other films suppressed differentiation, as shown in Table II. On the contrary, all condition mediums after 3-day cultivation did not show any enhancement of MB cell differentiation on a culture dish.

PC12 cells cultured with the condition medium from MB cell cultures showed little axonal growth after 1-wk incubation, and the axonal growth was similar among the various condition media of MB cells cultured on the different PE surfaces. On the other hand, the cells cultured with NGF showed strong axonal growth (data not shown), indicating that the con-

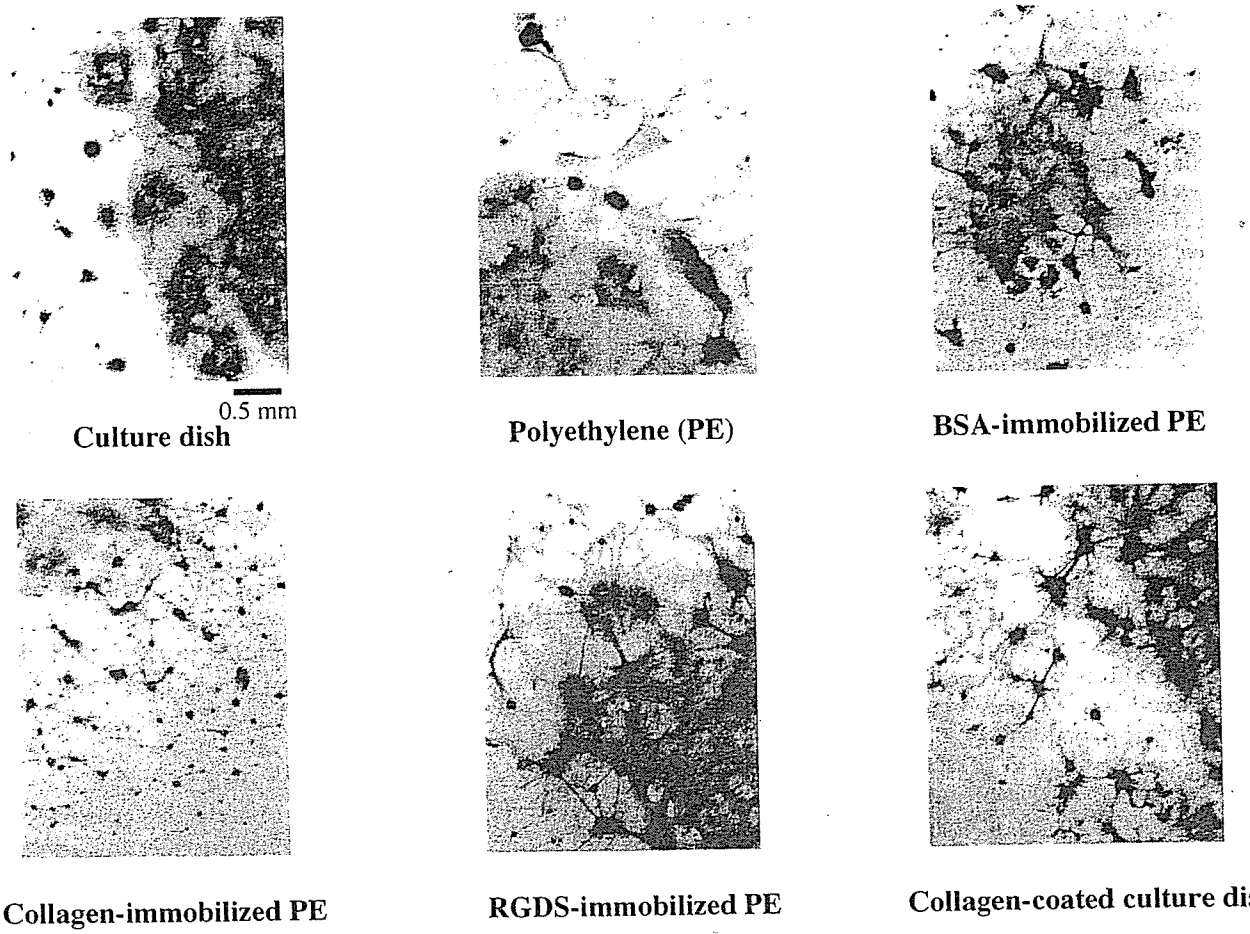

Figure 2. Light micrographs of Delafield's hematoxylin staining cultures of rat MB cells after incubation on various polyethylene surfaces.

dition medium does not contain a factor such as NGF that induces a differentiation of the PC12 cells directly.

DISCUSSION

Because function and differentiation of cells depend on circumstances such as the kinds of substrates, cell–substrate contact area, culture condition, and so on,[5–8] we should be very careful to choose the appropriate substrate for cell culture to achieve the desired function. We think this cell–substrate interaction is a very important, not only for basic cell studies but also for studies of hybrid-type artificial organs and tissue engineering. Therefore, in order to develop our tissue-engineering technique, we focused on effects of bio-

TABLE I
Effect of Surface Modification of Polyethylene Film by Protein Immobilization on Differentiation of Rat Midbrain Cells (mean value ± SD; $n = 4$)

	Culture Dish	Virgin PE	BSA-PE	Collagen-PE	RGDS-PE	Collagen-Coated Culture Dish
The amount of protein immobilized ($\mu g/cm^2$)	—	—	2.27	4.19	2.46	—[a]
Cytotoxicity (%)	100 ± 15.5	61.5 ± 9.0	75.5 ± 13.8	73.9 ± 38.3	43.4 ± 41.0	137 ± 10.6
The number of differentiated foci of MB cells	94.0 ± 16.6	67.0 ± 17.4	109 ± 26.5	159 ± 16.1**	168 ± 22.7**	174 ± 15.4[b]

[a]The coated amounts of collagen unknown.
[b]Significant difference observed among culture dish, PE, and BSA-PE.
*$p < 0.05$, **$p < 0.01$

TABLE II
Effect of Condition Media From Various MB Cell Culture Conditions on MB Cell Differentiation on a Collagen-Coated Culture Dish (mean value ± S.D. $n = 4$)

	Condition Medium Collected After	Condition Medium Collected From MB Culture				
		Collagen-Coated Culture Dish	PE	BSA-PE	Collagen-PE	RGDS-PE
Cytotoxicity (%)	3 days	100 ± 6.8	88.7 ± 9.4*	75.5 ± 13.8*	68.4 ± 9.9*	77.1 ± 15.2*
	7 days	100 ± 28.1	64.3 ± 15.9	39.1 ± 17.2**	50.5 ± 10.3*	42.7 ± 28.0**
Number of differentiated foci of MB cells	3 days	126 ± 12.3	109 ± 23.0	107 ± 6.4	100 ± 5.5	110 ± 10.4
	7 days	133 ± 9.3	105 ± 14.2*	90.0 ± 25.5*	133 ± 13.0	87.0 ± 61.8*

*$p < 0.05$, **$p < 0.01$ compared with a collagen-coated culture dish group or with group indicated.

materials on cell differentiation to estimate biocompatibility of materials. Moreover, we expected to find suitable cell scaffolds or substrates for inducing desirable function of targeted cells. In this study, PE film inhibited normal differentiation of MB cells cultured on it, and collagen and RGDS peptide immobilization onto PE surface resulted in an increased number of differentiated foci. In addition, MB cells on a collagen-coated culture plate showed more differentiated foci than those on a normal culture dish, as well as those observed on collagen-immobilized PE film. These results suggest that improvement of cell adhesion and cell proliferation by the immobilization of extracellular matrix protein promotes the differentiation of MB cells.

It has been reported that some materials show a potential to disrupt usual behavior of cells, resulting in undesirable effects on cells or tissues.[1,2,9–12] During these studies, we focused on the inhibitory activity of the materials on GJIC, which was found to play an important role in tumor promotion activity and correlated well with *in vivo* tumor potential.[10,11] In addition, GJIC plays an essential role in homeostasis maintenance by keeping many growth control signals at equilibrium among GJIC-connected cells and tissues.[13] Therefore, it is important to clarify the inhibitory activity of the materials on GJIC to estimate both their biocompatibility and their undesirable effects *in vivo*. In our previous study, PE film showed strong inhibitory activity on GJIC in metabolic cooperation assay systems. This inhibitory activity decreased when a surface of PE film was immobilized with extracellular matrix proteins such as collagen. However, surface modification of PE by immobilization of RGDS peptide, which plays an important role in cell adherence to the protein via integrin molecules on cell membrane, did not improve its inhibitory activity.[14] This result suggested that RGDS sequence in the protein was not sufficient to recover normal cell homeostasis via GJIC. Therefore, we expected that PE film immobilized with RGDS peptide would suppress normal cell differentiation of MB cells when cultured on the film, as well as on untreated PE film. This study showed that untreated PE film inhibited cell differentiation as expected. However, RGDS-immobilized PE showed a potential to differentiate the cells more than that on a control dish. There were many kinds of cells in this MB cell culture system, because primary cells collected from mouse embryos have been suggested to differentiate nerve cells on the layer of other cells, such as mesenchymal cells, in this system.[2] It is possible that growth of mesenchymal cells was improved by the surface modification with the cell-adhesive RGDS peptide, resulting in improved differentiation of the nerve cells. This suggests that interaction between mesenchymal cells normally grown on a substrate, and nerve cells on the layer of the mesenchymal cells, is one of the important factors in the differentiation of MB cells.

Through microscopic observations (Fig. 2), we observed that the number and size of MB cell foci on various kinds of PE films were different. For example, MB cell size was smallest when the cells were cultured on collagen-immobilized PE. On the other hand, when the MB cells were cultured on untreated PE film, the number of foci was fewer and, as observed, their size was larger than the foci seen on other films. In addition, many cell layers uniformly stained by hematoxylin were observed on the PE film. These findings indicate that MB cells could not gather to form foci when cultured on the PE film. However, improving the surface of the PE by protein immobilization recovered mobility of the cells to form the foci, judging from the microscopic observation. These results suggest that protein immobilization makes the surface more feasible for both cell movement and adherence. Considering this microscopic observation and data shown in Table II, it is probable that more nutrition is necessary for adhesion, movement, proliferation, and differentiation of MB cells on various kinds of PE films tested

rather than on a normal culture dish. Although further studies are needed, differences in surface characteristics of various PE films may cause different biological reactions in MB cells, resulting in different utilization of the nutrition in a culture medium.

Despite containing less nutrition, the condition medium from MB cell 7-day cultures on collagen-immobilized PE film might have the potential to improve differentiation of nerve cells, as shown in Table II. This suggests that the condition medium contains some factors that aid differentiation. Results from Table II also suggest that growth factors from the cells that aid differentiation may be secreted at least 3 days after starting MB cell culture, because the condition medium from 3-day cultures did not show any effects on differentiation. However, culture of PC12 cells in the condition medium indicated that growth factors in the medium had little NGF-like potential on differentiation. These results suggest the possibility of improving function of mesenchymal or nerve cells on the collagen-immobilized PE film to produce not NGF, but factors that may induce normal nerve cell differentiation, although the factors were not identified in this study. In addition, the condition medium from the 7-day cultures on other protein-immobilized films suppressed differentiation, although the number of differentiated foci directly on the films was more than that observed on PE film. This finding suggests that the condition medium did not contain the factors. In addition, this may also reflect lower nutrition in the condition medium than that taken from MB cell cultures on a normal culture dish. These results indicate that mechanisms of MB cell differentiation recovery on collagen-immobilized PE film are different from those of RGDS-immobilized PE. The hypothesis of MB cell differentiation on various PE films from the above findings is illustrated in Figure 3. Immobilization of protein makes a surface more hydrophilic. It is known that a hydrophobic or hydrophilic surface of biomaterials is one factor that affects cell adhesion behavior and function on them.[15] This change in surface characteristic can improve MB cell differentiation through normal adhesion and rearrangement of mesenchymal cells on PE surface. Because collagen and RGDS sequences can bind to a cell through integrins in the cell membrane, it is probable that the rearrangement of mesenchymal cells induces collagen- or RGDS-immobilized PE rather than BSA-immobilized PE. Moreover, collagen-immobilized PE, on which cells are reported to recover GJIC function, induces production of unknown factors that improve MB cell differentiation. Although we did not estimate directly the GJIC function of MB cells on various PE films, it is likely that the inhibitory activity of the PE films on the

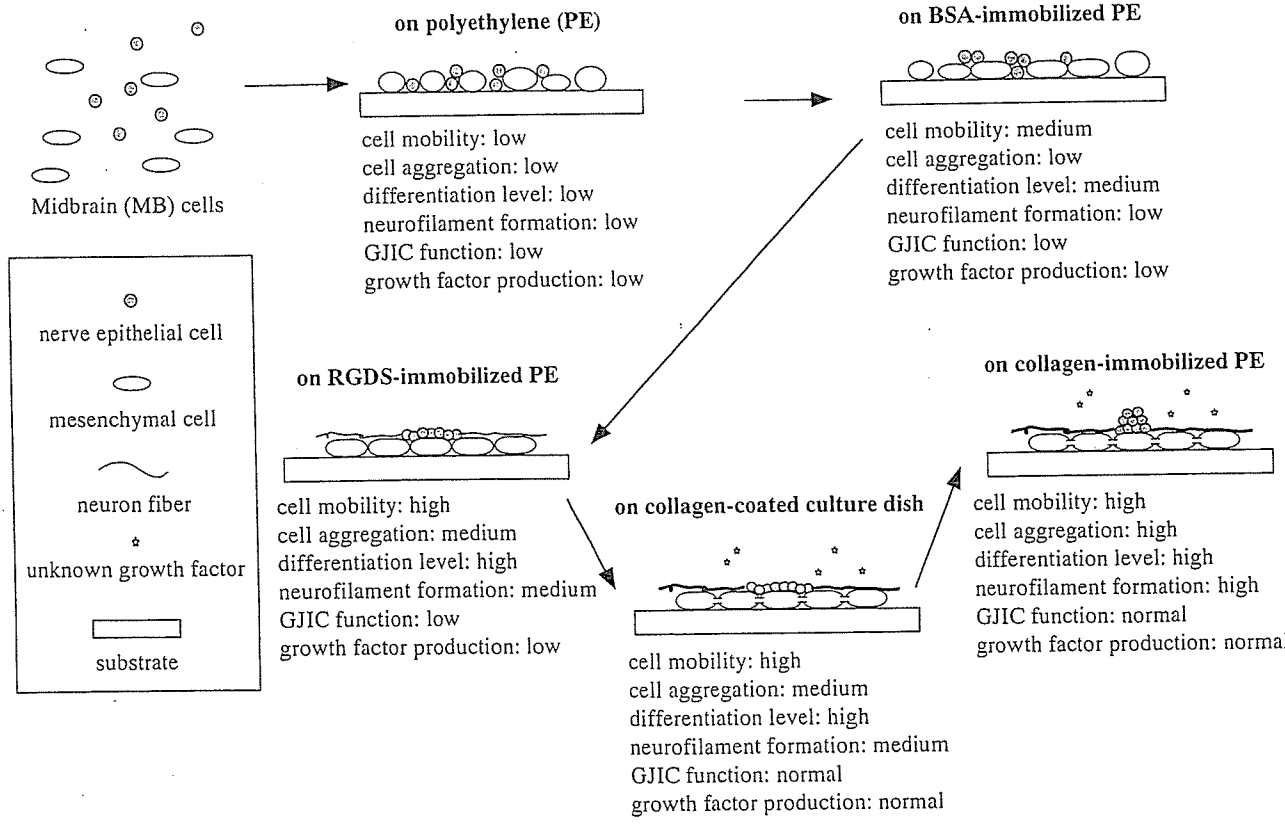

Figure 3. Schematic illustration of assumed differentiation mechanisms of MB nerve cells and mesenchymal cells after cultivation on various kinds of PE films.

GJIC relates to more or less production of the factors. Thus, MB cell differentiation may be affected by immobilized molecules through physicochemical feature of PE surface and recovery in the GJIC function of the mesenchymal cells. To prove this hypothesis about the specificity of the effects of immobilized molecule, it is indispensable to develop another experimental method with competitive chemicals binding to specific integrins.

Although collagen immobilization onto PE film increased differentiated foci of MB cells when cultured on the film, the number of the foci was comparable to that observed on a collagen-coated culture dish. As shown in Table I, however, proliferation of MB cells on the coated collagen is facilitated compared to that on the immobilized collagen. Therefore, there must be a difference in the effect of coated and immobilized collagen on the behavior of MB cells. As shown in Figure 2, the size and shape of the foci were different on the collagen-coated dish and collagen-immobilized PE. In addition, more nutrition was needed for MB cells on collagen-immobilized PE than for those on the collagen-coated dish, judging from the results shown in Table II, which suggests that MB cells on collagen-immobilized PE are more motile than those on the collagen-coated dish, resulting in their rearrangement into aggregated small foci (Figs. 2 and 3). Therefore, it is probable that the difference in MB cell behavior can be ascribed to a difference in molecular structure of coated collagen and immobilized collagen. Table II also indicated that the condition medium from collagen-immobilized PE had the potential to induce MB cell differentiation as well as that from the collagen-coated dish, although its cytotoxicity was higher. This suggests that MB cells on the immobilized PE produce unknown factors that improve their differentiation more than those on the coated dish. It has been reported that recovering GJIC function of dermal fibroblasts results in enhancement of growth factor production.[16] Therefore, it is probable that enhanced GJIC function of MB cells is induced by their aggregation. Although the amount of coated collagen on the dish is unknown, it is likely that immobilized collagen is suitable to prepare a surface for cell culture, biomaterials, scaffolds, and so on. To discuss different features of collagen-coated and collagen-immobilized surfaces for biomaterials more precisely, further studies, including an electrophysiological study of differentiated MB cells, are needed.

In conclusion, not only production of the factors but also direct interaction between the nerve cells and the mesenchymal cells may be responsible for the differentiation of MB cells. Moreover, it is probable that a surface characteristic of the biomaterial affects both the production and the interaction, as well as the GJIC function of cells on the surface. However, this study suggests that surface improvement of biomaterials for cell adherence is enough, in some cases, to maintain normal cell function and differentiation. Thus, a biomaterial surface should be carefully designed according to the purpose of the biomaterial.

The authors gratefully acknowledge Yoshito Ikada of Suzuka University of Medical Science, associate professor Koichi Kato and assistant professor Masaya Yamamoto of the Institute for Frontier Medical Science, Kyoto University, and Mr. Shojiro Matsuda of GUNZE Ltd. for their kind help with graft polymerization of acrylic acid monomers.

References

1. Nakaoka R, Tscuhiya T, Kato K, Ikada Y, Nakamura A. Studies on tumor-promoting activity of polyethylene: Inhibitory activity of metabolic cooperation on polyethylene surfaces is markedly decreased by surface modification with collagen but not with RGDS peptide. J Biomed Mater Res 1997;35:391–397.
2. Tsuchiya T, Eto K, Bürgin H, Kistler A. Micromass culture of midbrain cells and its relevance to *in vitro* mechanistic studies. Cong Anom 1992;32:105–116.
3. Tsuchiya T. A useful marker for evaluating tissue-engineered products: Gap-junctional communication for assessment of the tumor-promoting action and disruption of cell differentiation in tissue-engineered products. J Biomater Sci Polymer 2000;11: 947–959.
4. Rahman MS, Tsuchiya T. *In vitro* culture of human chondrocytes (1): A novel enhancement action of ferrous sulfate on the differentiation of human chondrocytes. Cytotechnology 2002. Forthcoming.
5. Wakabayashi Y, Sasaki J, Fujita H, Fujimoto K, Morita I, Murota S, Kawaguchi H. Effects of surface modification of materials on human neutrophil activation. Biochim Biophys Acta 1995;1243:521–528.
6. Nagahara S, Matsuda T. Cell-substrate and cell-cell interactions differently regulate cytoskeletal and extracellular matrix protein gene expression. J Biomed Mater Res 1996;32:677–686.
7. Kishida A, Kato S, Ohmura K, Sugimura K, Akashi M. Evaluation of biological responses to polymeric biomaterials by RT-PCR analysis. Biomaterials 1996;17:1301–1305.
8. Chen SC, Mrksich M, Huang S, Whitesides GM, Ingber DE. Geometric control of cell life and death. Science 1997;276:1425–1428.
9. Nakamura A, Kawasaki Y, Takeda K, Aida Y, Kurokawa Y, Kojima S, Shintani H, Matsui T, Nhomi T, Matsuoka A, Sofuni T, Kurihara M, Miyata N. Differences in tumor incidence and other tissue responses to polyetherurethanes and polydimethylsiloxane in long-term subcutaneous implantation into rats. J Biomed Mater Res 1992;26:631–650.
10. Tsuchiya T, Hata H, Nakamura A. Studies on the tumor-promoting activity of biomaterials: Inhibition of metabolic cooperation by polyetherurethane and silicone. J Biomed Mater Res 1995;29:113–119.
11. Tsuchiya T, Takahara A, Cooper SL, Nakamura A. Studies on the tumor-promoting activity of polyurethanes: Depletion of inhibitory action of metabolic cooperation on the surface of polyalkyleneurethane but not a polyetherurethane. J Biomed Mater Res 1995;29:835–841.
12. Tsuchiya T, Nakaoka R, Degawa H, Nakamura A. Studies on

the mechanisms of tumorigenesis induced by polyetherurethanes in rats: Leachable and biodegradable oligomers involving the diphenyl carbamate structure acted as an initiator on the transformation of Balb 3T3 cells. J Biomed Mater Res 1996;31:299–303.
13. Yamasaki H. Role of disrupted gap junctional intercellular communication in detection and characterization of carcinogens. Mutat Res 1996;365:91–105.
14. Nakaoka R, Tsuchiya T, Kato K, Ikada Y, Nakamura A. Studies on tumor-promoting activity of polyethylene: Inhibitory activity of metabolic cooperation on polyethylene surfaces is markedly decreased by surface modification with collagen but not with RGDS peptide. J Biomed Mater Res 1997;35:391–397.
15. Tamada Y, Ikada Y. Fibroblast growth on polymer surfaces and biosynthesis of collagen. J Biomed Mater Res 1994;28:783–789.
16. Park JU, Tsuchiya T. Increase of gap junctional intercellular communication by high molecular weight hyaluronic acid associated with FGF-2 and KGF-production in normal human dermal fibroblasts. Tissue Eng 2002. Forthcoming.

J Pharmacol Sci 93, 118 – 121 (2003)

Journal of Pharmacological Sciences
©2003 The Japanese Pharmacological Society

Short Communication

Block by Phytoestrogens of Recombinant Human Neuronal Nicotinic Receptors

Ken Nakazawa[1,*] and Yasuo Ohno[2]

[1]*Cellular and Molecular Pharmacology Section,* [1,2]*Division of Pharmacology, National Institute of Health Sciences, 1-18-1 Kamiyoga, Setagaya, Tokyo 158-8501, Japan*

Received June 5, 2003; Accepted July 2, 2003

Abstract. The effects of phytoestrogens on neuronal nicotinic acetylcholine receptor/channels were examined by expressing recombinant channels in *Xenopus* oocytes. When functional channels were expressed with human $\alpha 4$ and $\beta 2$ subuints, daidzein (10 and 100 μM) partially inhibited the ionic current activated by acetylcholine. The current inhibition was also observed when functional channels were expressed with human $\alpha 3$ and $\beta 4$ subunits or rat homologues. Genistin (100 μM) also inhibited the acetylcholine-activated current. Tamoxifen (100 μM), an antiestrogen did not antagonize the inhibition by daidzein. The results suggest that phytoestrogens, like estrogens and xenoestrogens, block human neuronal acetylcholine receptors through non-genomic mechanisms.

Keywords: human nicotinic receptor, phytoestrogen, non-genomic action

Phytoextrogens are estrogen-mimetic compounds involved in plants. Daidzein and genistein are isoflavonoid phytoestrogens occurring in beans (*Leguminosae*) including soybeans (*Glycine max*), red beans (*Phaseolus angularis*), and kudzu (*Pueraria lobata*). Because these beans are very popular foods, there have been warnings about the influence of the phytoestrogens as endocrine disruptors. In fact, it was reported that daidzein and genistein increased estrogen-specific human alkaline phosphatase activity (1). Phytoestrogens also exhibited estrogenic actions on bone metabolism (2) and vasodilation (3). On the other hands, beneficial effects of phytoestrogens against cardiovascular disease and cancer have been reported (4, 5). Neuroprotective effects of phytoestrogens have also been suggested from a cytotoxicity study in rat pheochromocytoma cells (6). We previously reported that estrogens and xenoestrogens modulate ionic current permeating through recombinant human neuronal nicotinic acetylcholine receptor/channel (7). The present study was aimed at clarifying whether or not phytoestrogens exhibit similar modulatory effects.

Cloned human and rat neuronal nicotinic receptors were expressed in *Xenopus* oocytes as described previously (8, 9). Defolliculated *Xenopus* oocytes were injected with in vitro transcribed cRNA's encoding α and β subunits and then incubated for 2 to 6 days at 18°C. Membrane current was measured by the conventional two-microelectrode voltage-clamp technique under the conditions described before (8). Oocytes were bathed in an experimental chamber of about 0.1 ml in volume filled with an extracellular solution [composition: 96 mM NaCl, 2 mM KCl, 1.8 mM $CaCl_2$, 1 mM $MgCl_2$, 5 mM HEPES, adjusted to pH 7.5 with NaOH] and held at −50 mV. A 400-ms hyperpolarizing voltage step to −80 mV was applied every 2 s to confirm clamp conditions. Acetylcholine and other substances were applied to oocytes by superfusion at a constant flow rate of about 0.5 ml/s. The application periods of acetylcholine were brief (6 to 10 s, depending on the concentrations of acetylcholine), and each application of acetylcholine was separated by 2 min. With this application protocol, stable inward current was activated by acetylcholine without obvious desensitization for 30 min or longer. Drugs used were acetylcholine chloride and tamoxifen (Sigma, St. Louis, MO, USA) and daidzein and genistin (Fujikko, Kobe). Tamoxifen, daidzein, and genistin were first dissolved in dimethylsulfoxide (DMSO). The final concentration of DMSO was 0.1% or 1%. DMSO at 0.1% or 1% did not affect the acetyl-

*Corresponding author. FAX: +81-3-3707-6950
E-mail: nakazawa@nihs.go.jp

choline-activated current. Oocytes were continuously exposed to tamoxifen, daidzein, or genistin 20 s before and during the application of acetylcholine. All the data were given as the mean ± S.E.M. Statistical analyses were made by the analysis of variance (ANOVA) followed by Tukey's test.

Figure 1A illustrates the ionic current activated by acetylcholine in an oocyte expressing human $\alpha 4$ and $\beta 2$ subunits. The acetylcholine-activated current was partially inhibited by 100 μM daidzein. The inhibition by 100 μM daidzein was statisitically significant (Fig. 1B). A lower concentration of daidzein (10 μM) did not significantly inhibit the acetylcholine-activated current. A higher concentration of daidzein (300 μM) could be not dissolved in 1% DMSO solution, so we were unable to test it. Figure 1C shows the dependence of inhibition on acetylcholine concentrations. The fraction blocked by 100 μM daidzein was larger when the current was activated by higher concentrations (1 and 10 mM) of acetylcholine than when it was activated by lower concentrations (10 and 100 μM).

Figure 2B compares the inhibition by daidzein of the acetylcholine-activated current recorded from oocytes expressing different subunit compositions. Daidzein (100 μM) inhibited the current permeating through human $\alpha 3\beta 4$ channel and rat $\alpha 3\beta 4$ channel as well as human $\alpha 4\beta 2$ channel. Similar tests were made with genistin, another isoflavonoid phytoestrogen that is glycosylated (Fig. 2A). Like daidzein, genistin (100 μM) inhibited acetylcholine-activated current permeating through the channels of all the three subunit compositions (Fig. 2C).

Effects of tamoxifen, an antiestrogen, on the current modulations by daidzein were examined. Daidzein (100 μM) also significantly inhibited the acetylcholine-activated current in the presence of 10 μM tamoxifen (Fig. 3).

The present study has demonstrated that two phytoestrogens (daidzein and genistin) inhibit recombinant neuronal nicotinic acetylcholine receptor/channels. The inhibition did not depend on subunit compositions (Fig. 2: B and C), as was the case with the inhibition by an artificial estrogen (diethylstilbestrol) or xenoestrogens (bisphenol A and *p*-nonylphenol) (7). The lack of dependence on subunit compositions suggests that the phytoestrogens interact with some region having a common structure among the different subunits or some constituent close to the channel proteins such as membrane lipids. In contrast, the modulations by other estrogens (17β-estradiol, 17α-estradiol, and 17α-ethynylestradiol) or a xenoestrogen (*p*-octylphenol) exhibited subunit-dependence (7). The inhibition by daidzein was not competitive because the inhibition

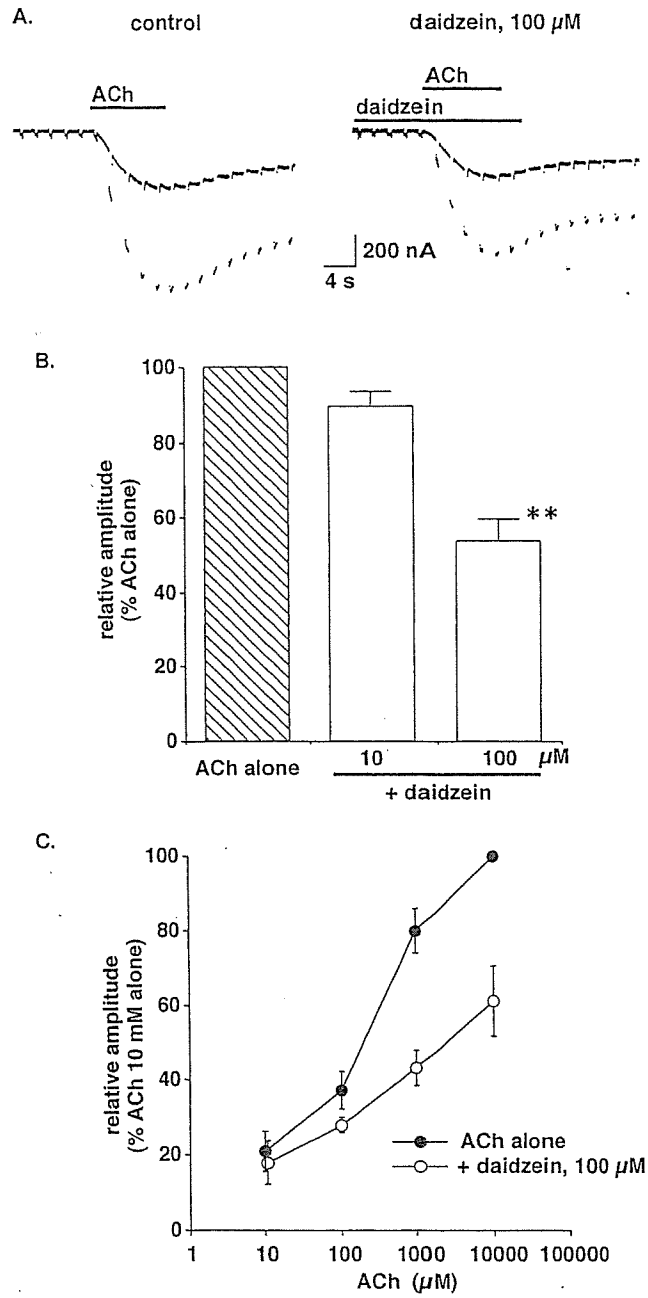

Fig. 1. Inhibition by daidzein of acetylcholine (ACh)-activated current. Functional channels consisting of human $\alpha 4$ and $\beta 2$ subunits were expressed in *Xenopus* oocytes. A: Inward current activated by 1 mM ACh in the absence (left) and presence (right) of 100 μM daidzein. The oocyte was held at −50 mV and stepped to −80 mV for 400 ms every 2 s. B: Summarized data. The current responses at −80 mV in the presence of 10 and 100 μM daidzein obtained as in panel A were normalized to those in the absence of daidzein in individual oocytes. Columns and bars are means and S.E.M. obtained from 5 oocytes. Asterisks indicate a significant difference from the current activated by ACh alone when absolute current amplitude was compared (**P<0.01). C: Concentration-response relationship for acetylcholine-activated current in the absence (filled circles) and presence of 100 μM daidzein (open circles). Symbol and bars represent means and S.E.M. obtained from 5 oocytes.

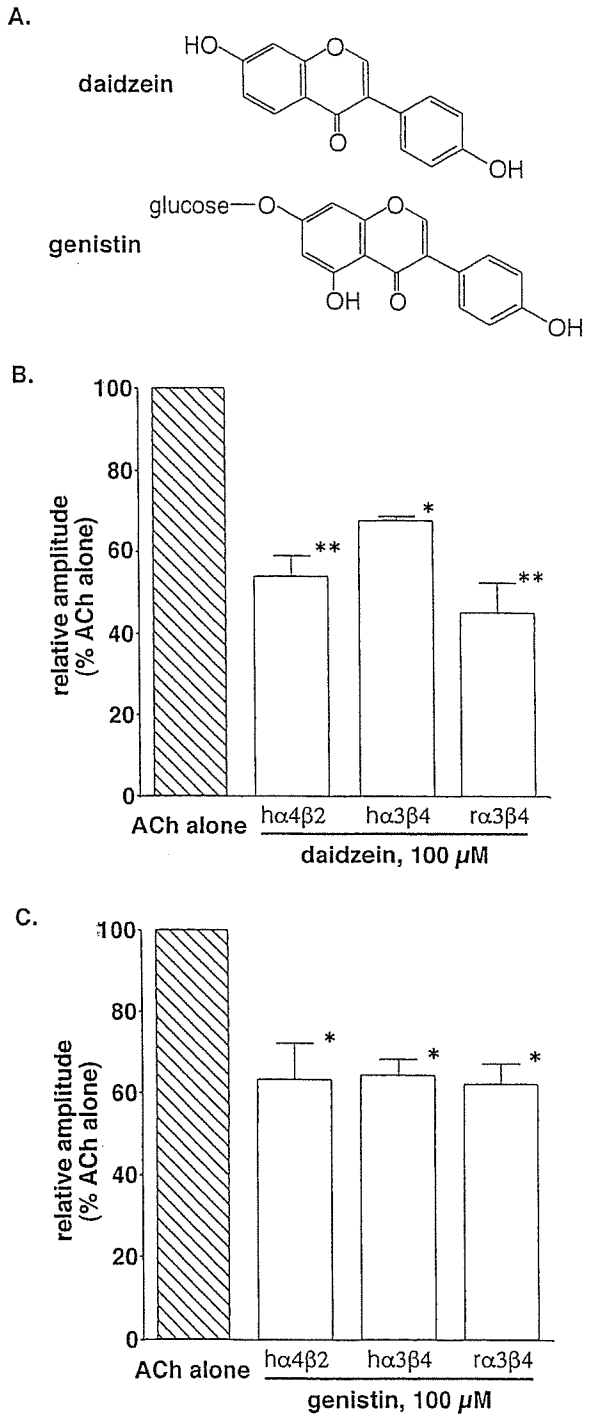

Fig. 2. Block by daidzein and genistin. A: Chemical structures of daidzein and genistin. B, C: Lack of remarkable subunit-dependence of block by daidzein (B) or genistin (C) of acetylcholine (ACh)-activated current. Functional channels were expressed with human $\alpha 4$ and $\beta 2$ subunits (h$\alpha 4\beta 2$), human $\alpha 3$ and $\beta 4$ subunits (h$\alpha 3\beta 4$), and rat $\alpha 3$ and $\beta 4$ subunits (r$\alpha 3\beta 4$). Inhibition by 100 μM daidzein or genistin of current activated by 1 mM (h$\alpha 4\beta 2$) or 100 μM (h$\alpha 3\beta 4$ and r$\alpha 3\beta 4$) ACh was tested as in Fig. 1A, and normalized current responses are shown as in Fig. 1B. Columns and bars are means and S.E.M. obtained from 5 oocytes. Asterisks indicate significant differences from current activated by ACh alone when absolute current amplitude was compared (*P<0.05, **P<0.01).

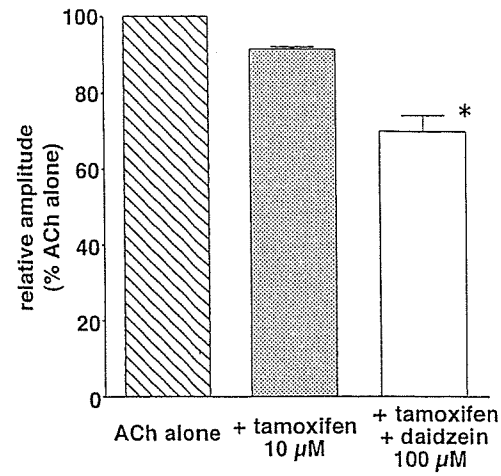

Fig. 3. Tamoxifen (10 μM) failed to antagonize block by 100 μM daidzein of 1 mM acetylcholine (ACh)-activated current. Functional channels were expressed with human $\alpha 4$ and $\beta 2$ subunits. Data were obtained and shown as in Fig. 1. Columns and bars are means and S.E.M. obtained from 5 oocytes. An asterisk indicates a significant difference from the ACh-activated current in the presence of tamoxifen when absolute current amplitude was compared (*P<0.05).

became larger when the concentration of acetylcholine was increased (Fig. 1C), which is opposite to decrease in inhibition along with increase of agonist concentration expected from competitive inhibition. The preferential block of the current activated by higher concentrations of acetylcholine suggests that daidzein binds to a special form of the nicotinic receptor. Another possibility is that interacellular Ca^{2+} concentration elevated by high acetylcholine concentrations is favorable for the block by daidzein. Non-competitive inhibition was observed with 17β-estradiol and other estrogen-minetic compounds (7). The inhibition by daidzein was not mediated through classical estrogen receptors or similar binding-sites because tamoxifen failed to suppress the inhibition (Fig. 3) at 10 μM, a concentration sufficient for blocking the classical estrogen receptors (e.g., Ref. 10). Inability of tamoxifen to suppress the current modulations was also found with other estrogens and xenoestrogens (7). For the inhibition, the hydroxyphenyl moiety of daidzein may be important because this moiety is shared by other compounds that modulate nicotinic acetylcholine receptors (for details, see discussion in Ref. 7). The conservation of the blocking potency of genistin, an analog glycosylated at the remaining moiety (Fig. 2: A and C) may support this view.

Dobrydneva et al. (11) reported that daidzein and other phytoestorgens block calcium influx in human platelets at 10 μM. The block of the nicotinic receptor reported here and that of calcium influx (11) are non-genomic actions because they are acute effects and

insensitive to antiestrogen. As for genomic actions, the estrogen-mimetic activity of isoflavonoid phytoestrogen has been reported to be 3 or 4 orders less potent than that of 17β-estradiol (1). 17β-Estradiol acts on estrogen receptors in the nanomolar concentration range (1 to 100 nM) (12). Thus, the genomic actions of phytoestrogens may occur at concentrations equivalent to those required for their non-genomic actions. According to the calculation of the amount of foods by Reinli and Block (1), this concentration range is readily attainable by daily meals. Thus, phytoestrogens may continuously affect the activity of acetycholine receptor/channels or other membrane proteins, which may result in neuronal modulations. It is, however, unclear at present whether this possible influence of phytoestrogens on neuronal systems is beneficial or risky.

Acknowledgments

This work was partly supported by Health and Labour Science Research Grants for Research on Advanced Medical Technology from the Ministry of Health, Labour and Welfare, Japan and a grant-in-aid for scientific research from the Ministry of Education, Culture, Sports, Science, and Technology, Japan (KAKENHI 13672319) awarded to K.N.

References

1 Reinli K, Block G. Phytoestrogen content of foods — a compendium of literature values. Nutr Cancer. 1996;26:123–148.
2 Tsutsumi N, Kawashima K, Nagata H, Ujiie A, Endo H. Effects of KCA-012 on bone metabolism in organ culture. Jpn J Pharmacol. 1995;67:169–171.
3 Yamaguchi K, Honda H, Wakisaka C, Tohei A, Kogo H. Effects of phytoestrogens on acetylcholine- and isoprenaline-induced vasodilation in rat aorta. Jpn J Pharmacol. 2001;87:67–73.
4 Bolego C, Poli A, Cignarella A, Paoletti R. Phytoestrogens: pharmacological and therapeutic perspectives. Curr Drug Targets. 2003;4:77–87.
5 Kris-Etherton PM, Hecker KD, Bonanome A, et al. Bioactive compounds in foods: their role in the prevention of cardiovascular disease and cancer. Am J Med. 2002;113 Suppl 9B:71S–88S.
6 Gelinas S, Martinoli MG. Neuroprotective effect of estradiol and phytoestrogens on MPP^+-induced cytotoxicity in neuronal PC12 cells. J Neurosci Res. 2002;70:90–96.
7 Nakazawa K, Ohno Y. Modulation by estrogens and xenoestrogens of recombinant human neuronal nicotinic receptors. Eur J Pharmacol. 2001;430:175–183.
8 Nakazawa K, Akiyama T, Inoue K. Block by apomorphine of acetylcholine receptor channels expressed in *Xenopus* oocytes. Eur J Pharmacol. 1994;269:375–379.
9 Nakazawa K, Ohno Y. Block by 5-hydroxytryptamine and apomorphine of recombinant human neuronal nicotinic receptors. Eur J Pharmacol. 1999;374:293–299.
10 Singer CA, Rogers KL, Strickland TM, Dorsa DM. Estrogen protects primary cortical neurons from glutamate toxicity. Neurosci Lett. 1996;212:13–16.
11 Dobrydneva Y, Williams RL, Morris GZ, Blackmore PF. Dietary phytoestrogens and their synthetic structural analogues as calcium channel blockers in human platelets. J Cardiovasc Pharmacol. 1999;40:399–410.
12 Nishikawa J, Saito K, Goto J, Dakeyama F, Matsuo M, Nishihara T. New screening methods for chemicals with hormonal activities using interaction of nuclear hormone receptor with coactivator. Toxicol Appl Pharmacol. 1999;154:76–83.

Available online at www.sciencedirect.com
SCIENCE DIRECT®
European Journal of Pharmacology 474 (2003) 205–208
ejp
www.elsevier.com/locate/ejphar

Short communication

Intracellular disulfide bond that affects ATP responsiveness of $P2X_2$ receptor/channel

Ken Nakazawa[a,*], Hiloe Ojima[a,b], Reiko Ishii-Nozawa[b], Koichi Takeuchi[b], Yasuo Ohno[c]

[a] *Cellular and Molecular Pharmacology Section, Division of Pharmacology, National Institute of Health Sciences, 1-18-1 Kamiyoga, Setagaya, Tokyo 158-8501, Japan*
[b] *Department of Clinical Pharmacology, Meiji Pharmaceutical University, Kiyose, Tokyo 204-8588, Japan*
[c] *Division of Pharmacology, National Institute of Health Sciences, 1-18-1 Kamiyoga, Setagaya, Tokyo 158-8501, Japan*

Received 20 March 2003; received in revised form 20 June 2003; accepted 27 June 2003

Abstract

The role of intracellular cysteine residues in $P2X_2$ receptor/channel was investigated. When dithiothreitol was intracellularly applied, both the maximal response and the sensitivity of the wild-type channel to ATP were decreased. On the other hand, Cu^{2+} phenanthroline did not affect the responsiveness. When two intracellular cysteine residues (Cys^9 and Cys^{430}) were replaced with alanine, both the maximal response and the sensitivity was decreased with the replacement at Cys^9, whereas no such decrease was observed with the replacement at Cys^{430}. These results suggest that an intracellular disulfide bond involving Cys^9 regulates the responsiveness of $P2X_2$ receptor/channel to ATP.
© 2003 Elsevier B.V. All rights reserved.

Keywords: ATP; P2X receptor; Site-directed mutagenesis; Cysteine; *Xenopus* oocyte

1. Introduction

P2X receptors are ion-channel-forming membrane proteins that are activated by extracellular ATP (see reviews of Ralevic and Burnstock, 1998; Khah, 2001; North, 2002). One functional ion channel is presumably formed by three homogeneous subunits. Each subunit has two transmembrane regions, a long extracellular loop between them, a short intracellular N-terminal region and a relatively long intracellular C-terminal region. Intracellular cysteine residues involved in cyclic nucleotide-gated ion channels have been shown to modulate the responsiveness to cGMP and cAMP (Gordon et al., 1997; Rosenbaum and Gordon, 2002). $P2X_2$ receptor contains two intracellular cysteine residues: one is in the N-terminal region (Cys^9) and the other is in the C-terminal region (Cys^{430}). In the present study, we investigated the roles of these intracellular cysteine residues in the responsiveness of $P2X_2$ receptor to ATP.

2. Material and methods

The expression of $P2X_2$ receptor and its mutants and the recordings of ionic current through the channels were performed according to our previous reports (Nakazawa et al., 1998, 1999). Briefly, $P2X_2$ receptor mutants were constructed from the cloned $P2X_2$ receptor (Brake et al., 1994) by site-directed mutagenesis. The wild-type and the mutant channels were expressed in *Xenopus* oocytes for a 4-day incubation at 18 °C, and the oocytes were served for membrane current recordings. Oocytes were bathed in ND96 solution containing (in mM) NaCl 96, KCl 2, $CaCl_2$ 1.8, $MgCl_2$ 1, HEPES 5 (pH 7.5 with NaOH). ATP (adenosine 5′ -triphosphate disodium salt; Sigma, St. Louis, MO, USA) was applied by superfusion for about 6 s with a regular interval of 1 min. Intracellular application of dithiothreitrol or other agents was made by injection 30 min prior to current recordings. About a one-hundredth of oocyte volume (50 nl) of 100× solutions were injected. Cu^{2+} phenanthroline (Kobayashi, 1968) was prepared from cupric sulfate and phenathroline according to Rosenbaum and Gordon (2002). Cu^{2+} phenanthroline and iodine was first prepared in ethanol as 1000× solutions, diluted to 100× solutions with distilled water. Dithiothreitrol was dissolved in distilled water. The expected final concentrations are 2

* Corresponding author. Tel.: +81-3-3700-9704; fax: +81-3-3707-6950.
E-mail address: nakazawa@nihs.go.jp (K. Nakazawa).

0014-2999/03/$ - see front matter © 2003 Elsevier B.V. All rights reserved.
doi:10.1016/S0014-2999(03)02038-7

mM (dithiothreitrol), 1.5 μM (cupric sulfate), 5 μM (phenanthroline) and 300 μm (iodine), respectively. Statistical analysis was made by two-tailed Student's *t*-test with Welch's correction or the analysis of variance (ANOVA) followed by Tukey's test. Statistical significance was judged when $P<0.05$.

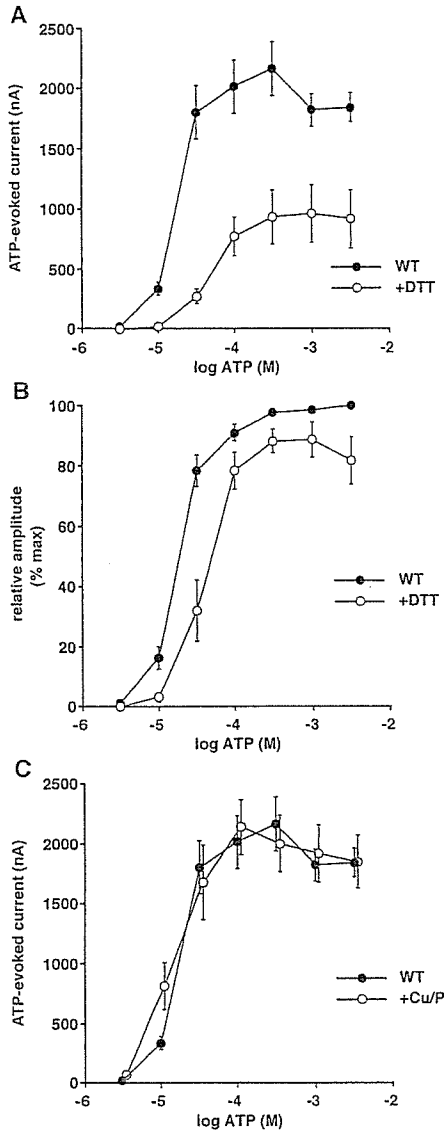

Fig. 1. Effects of dithiothreitrol and Cu^{2+} phenanthroline on ionic current evoked by ATP mediated through the wild-type $P2X_2$ receptor/channel expressed in *Xenopus* oocytes. Oocytes were held at −50 mV. Each symbol and bar represents the mean and S.E. obtained from five to seven oocytes tested. (A) Concentration–response relationship for the ATP-evoked current through the wild-type $P2X_2$ receptor/channel. The data from dithiothreitrol-injected oocytes (+DTT) were compared with those from untreated oocytes (WT). (B) Normalized current responses plotted against ATP concentrations. The data shown in (A) were normalized to maximal responses to ATP in individual oocytes. (C) Concentration–response relationship obtained from Cu^{2+} phenanthroline-injected oocytes (+Cu/P) compared with that from uninjected oocytes (WT). Absolute current responses were plotted against ATP concentrations.

3. Results

Fig. 1A compares the concentration–response relationships for ionic current through the wild-type $P2X_2$ receptor/channel activated by ATP at −50 mV in dithiothreitrol-injected oocytes with that in uninjected oocytes. In the dithiothreitrol-injected oocytes, the maximal amplitude of ATP-evoked current was about a half as large as that in the uninjected oocytes. The current amplitude was significantly smaller in the dithiothreitrol-injected oocytes than in the uninjected oocytes at ATP concentrations of 10 μM and higher (Welch's test). The sensitivity to ATP was compared by plotting normalized current amplitude against ATP concentrations (Fig. 1B). The concentration–response relationship was about threefold shifted to right by the dithiothreitrol injection. The normalized current amplitude was significantly smaller in the dithiothreitrol-injected oocytes than in the uninjected oocytes at ATP concentrations of 10 and 30 μM (Welch's test). The current response obtained from Cu^{2+} phenanthroline-injected oocytes was not different from that from uninjected oocytes (Fig. 1C). The current response was also unaffected by iodine injection (not shown).

Fig. 2 compares the concentration–response relationship for the ATP-activated current in oocytes expressing the wild-type channel and those expressing cysteine-to-alanine substituted mutants (substitution at Cys^9 alone, Cys^{430} alone, or both Cys^9 and Cys^{430}). With the substitution at Cys^{430}, the maximal response (Fig. 2A) and the sensitivity to ATP (Fig. 2B) were not changed. On the other hand, remarkable changes were observed with the substitution at Cys^9: the maximal response was decreased by 60% (Fig. 2A) and the sensitivity was lowered by about threefold (Fig. 2B). Significant difference was found for the absolute current amplitude (Fig. 2A) at ATP concentrations at 10 μM and higher, and it was found for the normalized current amplitude (Fig. 2B) at ATP concentrations from 10 to 100 μM (Tukey's test). Introduction of the second mutation at Cys^9 did not add further decrease in the responsiveness to ATP (Fig. 2A and B). Effects of dithiothreitrol and Cu^{2+} phenanthroline on the Cys^9-to-alanine substituted channel were tested. Dithiothreitrol did not decrease the maximal current response through the Cys^9-to-alanine substituted channel (Fig. 2C), in contrast to a remarkable decrease in the maximal current response through the wild-type channel (Fig. 1A). Dithiothreitrol did not change the sensitivity of the Cys^9-to-alanine substituted channel to ATP (Fig. 2D). Cu^{2+} phenanthroline affected neither the maximal current response nor the sensitivity to ATP (Fig. 2C and D).

4. Discussion

The responsiveness of $P2X_2$ receptor was decreased by a reduction agent dithiothreitrol but not by oxidation agents Cu^{2+} phenanthroline or iodine. When cysteine-to-alanine substitution was made, a similar decrease of the

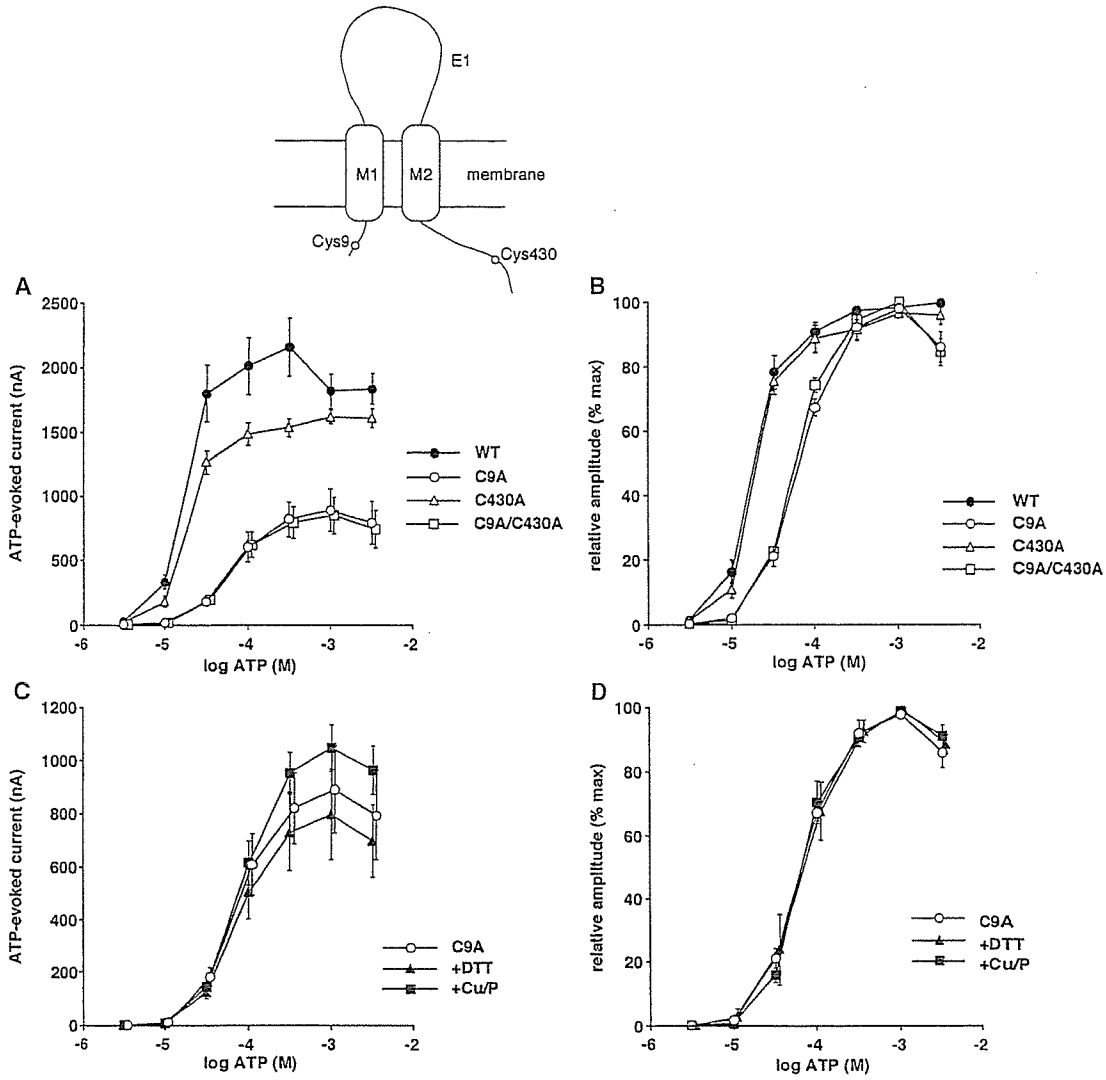

Fig. 2. Responses of cysteine-to-alanine mutants to ATP. Oocytes were held at −50 mV. Each symbol and bar represents the mean and S.E. obtained from five to seven oocytes tested. (A) Concentration–response relationship for ATP-evoked current mediated through the wild-type $P2X_2$ receptor/channel (WT) and three cysteine-to-alanine mutants (substitution at Cys^9 alone, Cys^{430} alone or both Cys^9 and Cys^{430}; C9A, C430A and C9A/C430A, respectively). (B) Normalized current responses. The data shown in (A) were normalized to maximal responses to ATP in individual oocytes. (C) ATP-evoked current mediated through the Cys^9-to-alanine substituted mutant channel. Concentration–response relationship obtained from dithiothreitrol- (+DTT) and Cu^{2+} phenanthroline-injected oocytes (+Cu/P) was compared with that from uninjected oocytes (C9A). (D) Normalized current responses. The data shown in (C) were normalized to maximal responses to ATP in individual oocytes.

responsiveness to ATP was observed in the Cys^9-to-alanine mutant channel, and dithiothreitrol did not produce a further decrease in the responsiveness in this mutant. These results suggest that an intracellular disulfide bond is necessary for the physiological responsiveness of $P2X_2$ receptor to ATP, and that Cys^9 participates in this disulfide bond. In rat $P2X_1$ receptor, multimerization of homomeric receptor subunits has been shown to be decomposed by dithiothreitrol (Nicke et al., 1998). A larger part of this multimerization seems to be achieved by non-disulfide bonds because the decomposition to monomers occurs even without reduction agents. A smaller part of the multimerization, however, appears to be achieved by disulfide bonds because $P2X_1$ oligomers up to hexamers do not completely disappear in the absence of dithiothreitrol. Cysteine residues are not found in the intracellular N- or C-terminal region of rat $P2X_1$ receptor (Soto et al., 1997). Our finding of the modification by an intracellular disulfide bond may not be applicable to other P2X receptor subclasses including rat $P2X_1$, $P2X_5$ and $P2X_6$ receptors that lack corresponding cysteine residues. Unlike intracellular cysteine residues, extracellular cysteine residues are highly conserved among P2X subclasses. The pairs of cysteines that form disulfide bonds have been identified for $P2X_1$ (Ennion and Evans, 2002) and $P2X_2$ receptors (Clyne et al., 2002), recently.

In cyclic nucleotide-gated channels, disulfide bonds also modulate the sensitivity to agonists, namely, intracellular

cGMP and cAMP (Gordon et al., 1997; Rosenbaum and Gordon, 2002). The formation of the disulfide bond between Cys^{35} of the N-terminal region and Cys^{481} of the C liker region increases the responsiveness to cGMP and cAMP. These Cys^{35} and Cys^{481} are normally reduced, and oxidation agents (Cu^{2+} phenanthroline and iodine) enhance the channel activation. In contrast to the cysteine residues in the cyclic nucleotide-gated channel, Cys^{9} in $P2X_2$ receptor is normally oxidized and the reduction appears to result in decrease in the responsiveness to ATP. The counterpart of the disulfide bond may not be the other intracellular cysteine residue Cys^{430} because the replacement of Cys^{430} did not change the responsiveness to ATP (Fig. 2A and B). Because P2X receptors are believed to form trimers, a disulfide bond may be made intermolecularly between subunits. If this is the case, one disulfide bond may be formed between two of three subunits in one homomeric receptor. The remaining subunit may stay unbound or bind to some protein intrinsically expressed in or beneath cell membrane in *Xenopus* oocytes. Other possibilities including binding of individual subunits to domain proteins through three disulfide bonds cannot be excluded.

Acknowledgements

This work was partly supported by Health and Labour Science Research Grants for Research on Advanced Medical Technology and Research on Environmental Health from the Ministry of Health, Labour and Welfare, Japan, awarded to Y.O. and K.N., and a grant-in-aid for scientific research from the Ministry of Education, Science, Sports and Culture, Japan (KAKENHI 13672319), awarded to K.N.

References

Brake, A.J., Wagenbach, M.J., Julius, D., 1994. New structural motif for ligand-gated ion channels defined by an ionotropic ATP receptor. Nature 371, 519–523.

Clyne, J.D., Wang, L.-F., Hume, R.I., 2002. Mutational analysis of the conserved cysteines of the rat $P2X_2$ purinoceptor. J. Neurosci. 22, 3873–3880.

Ennion, S.J., Evans, R.J., 2002. Conserved cysteine residues in the extracellular loop of the human $P2X_1$ receptor form disulfide bonds and are involved in receptor trafficking to the cell surface. Mol. Pharmacol. 61, 303–311.

Gordon, S.E., Varnum, M.D., Zagotta, W.N., 1997. Direct interaction between amino- and carboxyl-terminal domains of cyclic nucleotide-gated channels. Neuron 9, 4331–4441.

Khah, B.S., 2001. Molecular physiology of P2X receptors and ATP signalling at synapses. Nat. Rev. 2, 165–174.

Kobayashi, K., 1968. Catalytic oxidation of sulfhydryl groups by *o*-phenathroline copper complex. Biochim. Biophys. Acta 158, 239–245.

Nakazawa, K., Ohno, Y., Inoue, K., 1998. An aspartic acid residue near the second transmembrane segment of ATP receptor/channel regulates agonist sensitivity. Biochem. Biophys. Res. Commun. 244, 599–603.

Nakazawa, K., Inoue, K., Ohno, Y., 1999. Block and unblock by imipramine of cloned and mutated P2X2 receptor/channel expressed in Xenopus oocytes. Neurosci. Lett., 93–96.

Nicke, A., Bäumert, G., Rettinger, J., Eichele, A., Lambrecht, G., Mutschler, E., Schmalzing, G., 1998. $P2X_1$ and $P2X_3$ receptors form stable trimers: a novel structural motif of ligand-gated ion channels. EMBO J. 17, 3016–3028.

North, R.A., 2002. Molecular physiology of P2X receptors. Physiol. Rev. 82, 1013–1067.

Ralevic, V., Burnstock, G., 1998. Receptors for purines and pyrimidines. Pharmacol. Rev. 50, 413–492.

Rosenbaum, T., Gordon, S.E., 2002. Dissecting intersubunit contacts in cyclic nucleotide-gated ion channels. Neuron 33, 703–713.

Soto, F., Garcia-Guzman, M., Stühmer, W., 1997. Cloned ligand-gated channels activated by extracellular ATP (P2X receptors). J. Membr. Biol. 160, 91–100.

ELSEVIER

FEMS Microbiology Ecology 44 (2003) 253–259

FEMS MICROBIOLOGY Ecology

www.fems-microbiology.org

Ultrastructural changes in *Chlamydomonas acidophila* (Chlorophyta) induced by heavy metals and polyphosphate metabolism

Kahoko Nishikawa [a,*], Yoko Yamakoshi [b], Isao Uemura [c], Noriko Tominaga [a]

[a] *Institute of Environmental Science for Human Life, Ochanomizu University, 2-1-1 Otsuka, Bunkyo-ku, Tokyo 112-8610, Japan*
[b] *Division of Organic Chemistry, National Institute of Health Sciences, 1-18-1 Kamiyoga, Setagaya, Tokyo 158-8501, Japan*
[c] *Department of Biology, Tokyo Metropolitan University, 1-1 Minamiohsawa, Hachioji, Tokyo 192-0397, Japan*

Received 24 September 2002; received in revised form 26 December 2002; accepted 6 January 2003

First published online 15 February 2003

Abstract

Ultrastructural changes induced by heavy metals (cadmium, zinc, and copper) and polyphosphate metabolism were studied in *Chlamydomonas acidophila*. Transmission electron microscopy indicated that cadmium led to the most drastic morphometric changes. An increase in number and volume of starch grains and vacuoles as well as the presence of electron dense deposits in vacuole and membrane whorls were observed. Energy-dispersive X-ray analysis revealed that vacuolar deposits inside cells treated with cadmium contained phosphate and cadmium. These ultrastructural changes were accompanied by a change in the intracellular polyphosphate level, as shown by in vivo ^{31}P-nuclear magnetic resonance. It was also observed that cadmium treatment caused polyphosphate degradation and increased vacuolar short-chains and orthophosphates.
© 2003 Federation of European Microbiological Societies. Published by Elsevier Science B.V. All rights reserved.

Keywords: heavy-metal detoxification; Cd; Polyphosphate; Algae; Ultrastructure

1. Introduction

Acidification of the environment by acid rain has adverse effects on ecological systems. Some reports show that a shift in pH from neutral to acidic causes a reduction in algal and fish population. Sulfuric acid directly results in poor production of fish eggs, with production of spines and other deformities [1,2]. Indirectly, lower pH induced by acid rain is accompanied by an increase in metal ion concentration in soil and aquatic environments and acidification leads to leaching of poisonous metals such as aluminum, cadmium and mercury, from the soil. A close relationship exists between metal toxicity and pH in soil and aquatic environments.

Chlamydomonas acidophila, isolated from Lake Katanuma in Japan, has adapted to acidic environmental stress (acidification and heavy-metal toxicity) [3]. In particular, we studied the mechanism of heavy-metal detoxification in *C. acidophila*, because heavy-metal contamination of the environment is a severe problem with consequences throughout the food chain.

Heavy-metal concentrations in the environment have increased due to industrial activity and acid rain. For example, Cd usage has increased in plastic manufacturing, electroplating of steel, Ni–Cd batteries and in pigments [4].

In this study, the mechanism of heavy-metal detoxification was studied in *C. acidophila* by observing ultrastructural damage. Additionally, we focused on phosphate metabolism and metal detoxification because energy-dispersive X-ray (EDX) analysis on *C. acidophila* suggested a close relationship with metal detoxification.

We estimated ultrastructural damage using morphometric analysis. Electron microscope morphometric techniques can be used to quantitatively assess the impact of perturbations on cytological characteristics in their natural environment [5]. The detoxification of heavy metals is accomplished by several different cellular mechanisms: exclusion, precipitation, reduction, and active transport. This alga may have another detoxification mechanism, in addition to the metallothionein and phytochelatin. This mechanism

* Corresponding author. Tel.: +81 (3) 5978 5809; Fax: +81 (3) 5978 5804.
E-mail address: kaho@jk9.so-net.ne.jp (K. Nishikawa).

0168-6496/03/$22.00 © 2003 Federation of European Microbiological Societies. Published by Elsevier Science B.V. All rights reserved.
doi:10.1016/S0168-6496(03)00049-7

will help the understanding of adaptation to acidified environments in other organisms.

2. Materials and methods

2.1. Culture condition

Stocks of the green alga, *C. acidophila* (Chlorophyta), were grown as previously described [3]. Axenic cultures were maintained by periodic transfers in modified Sager–Granick Medium [6] (1.22 mM $MgSO_4 \cdot 7H_2O$, 3.75 mM NH_4NO_3, 0.57 mM K_2HPO_4, 0.73 mM KH_2PO_4, 0.36 mM $CaCl_2$, 37 μM $FeCl_3 \cdot 6H_2O$, 16.2 μM H_3BO_4, 3.5 μM $ZnSO_4 \cdot H_2O$, 2.02 μM $MnCl_2 \cdot 4H_2O$, 0.24 μM $CuSO_4 \cdot 5H_2O$, 0.84 μM $CoCl2 \cdot 6H_2O$, 0.83 μM $Na_2MoO_4 \cdot H_2O$, 50 mM succinic acid, with pH adjusted to 4.0 by addition of 1 N HCl). Cells were grown at 20°C, with 146 mE m^{-2} s^{-1} of illumination and a 12 h/12 h light/dark cycle. All glassware was washed with HCl and media and glassware were sterilized by standard autoclave procedures.

2.2. Metal treatment

Effective concentrations of cadmium, copper and zinc were achieved by reducing the population growth of *C. acidophila* to 50% of the control values (EC_{50}) obtained from the 72-h static exposure tests. Static metal treatment was carried out for 3 days with the addition of EC_{50} concentration, as previously reported [3]. In short, a modified Sager–Granick medium, pH 4, was used for the metal treatment with the addition of the following nominal metals at the concentrations: 20 μM $3CdSO_4 \cdot 6H_2O$, 200 μM $CuCl_2 \cdot 2H_2O$, and 1.5 mM $ZnCl_2$. Cells were grown as described above.

2.3. Morphometric analysis

For studies where techniques of morphometric analysis were used, the cultures were exposed for 72 h to three metals as described above. After the metal treatment, the cells were harvested and fixed with 1.0% glutaraldehyde in 50 mM acetate buffer for 20 min at room temperature. Fixed samples were washed 10 times with acetate buffer (pH 4) and post-fixed with 2% OsO_4 overnight at 4°C.

Samples were washed with acetate buffer, dehydrated in a graded ethanol series and embedded in Epon 812. Ultrathin sections were stained in aqueous 1% (w/v) uranyl acetate and lead citrate. Transmission electron micrographs (TEM) were obtained by JEOL-1230 electron microscope using an accelerating voltage of 60 kV. The sections of a cell were selected at random and photographed.

Following general techniques for modified morphometric analysis [7–11], cellular features, including whole cell, cytoplasm, chloroplast, vacuole, starch grains, pyrenoid, nucleus and mitochondria, have been analyzed. Over 20 microphotographs were scanned (Epson GT-7200U), each representing a separate cell, and analyzed (NIH image program) to determine the area of each organelle for each of the test conditions. The mean and standard error were obtained for each measurement and significance of the differences was determined by one-way analysis of variance (ANOVA).

2.4. Accumulation of Cd

Accumulations of Cd were measured using an Atomic Absorption Spectrophotometer (AA-660, Shimazu). Cells, treated with 10 or 20 μM Cd for 1, 2, and 3 days, were collected by centrifugation and washed three times with 0.1 M ethylenediamine tetraacetic acid (EDTA). Samples were dried and digested with a mixed acidic solution of HNO_3 and $HClO_4$ (9:1) for 12 h at 100°C. Samples were diluted with 1 N HCl and analyzed for Cd content. Protein levels were analyzed using the BCA method (Shigma).

2.5. EDX analysis

EDX analysis was performed at the electron microscopy center of Tokyo Metropolitan University. Specimen grids were examined by a Hitachi H 710 FA transmission electron microscope at an accelerating voltage of 80 kV. Fine probe size was adjusted to cover the vacuolar deposits, and X-rays were collected for 100 s utilizing a thin window detector. Carbon-coated copper grids supported the thin sections.

2.6. ^{31}P-NMR (nuclear magnetic resonance) measurement

^{31}P-NMR measurements were performed using a Varian XL-400 spectrometer operated at 162 MHz with a sweep width of 32362 Hz. The free induction decay was performed with a line broadening of 10 Hz. Pulses with a flip angle of 60° and repetition rate of 0.5 s were used. The cells were measured at room temperature in a 5-mm-diameter probe head. All chemical shifts were measured in ppm using triphenylphosphate as an external standard. Chemical shifts were measured relative to an external standard of 85% orthophosphoric acid. It is reported that the ratio of polyphosphate to orthophosphate in vacuoles is growth-dependent [12]; it was measured in 6-day-old (exponential phase) cells. Cells in the exponential phase of growth were transferred to a medium containing 20 μM Cd for 3 days (Cd-treated) and then retransferred to a non-metal medium for 3 days (recovered cells). Measurements were performed on untreated cells, Cd-treated cells and recovered cells. Cells were harvested by centrifugation, washed in phosphate-free 50 mM *N*-2-hydroxyethylpiperazine-*N'*-2-ethanesulfonic acid (HEPES) at pH 4.0, and suspended in the same buffer to a cell concentration of approximately 10^9 cells ml^{-1}.

3. Results

3.1. Effects of heavy metals on ultrastructure

The structural damage due to exposure to each metal was distinctly different. When treated with Cd, the whole cell size increased compared to untreated cells (Fig. 1a,b). On the other hand, cells treated with Cu and Zn decreased in size while maintaining their ellipsoidal shape (Fig. 1c,d).

Detailed morphometric analyses of the Cd, Cu and Zn treatments are presented in Table 1. As shown therein, 20 μM Cd caused the most drastic morphometric changes.

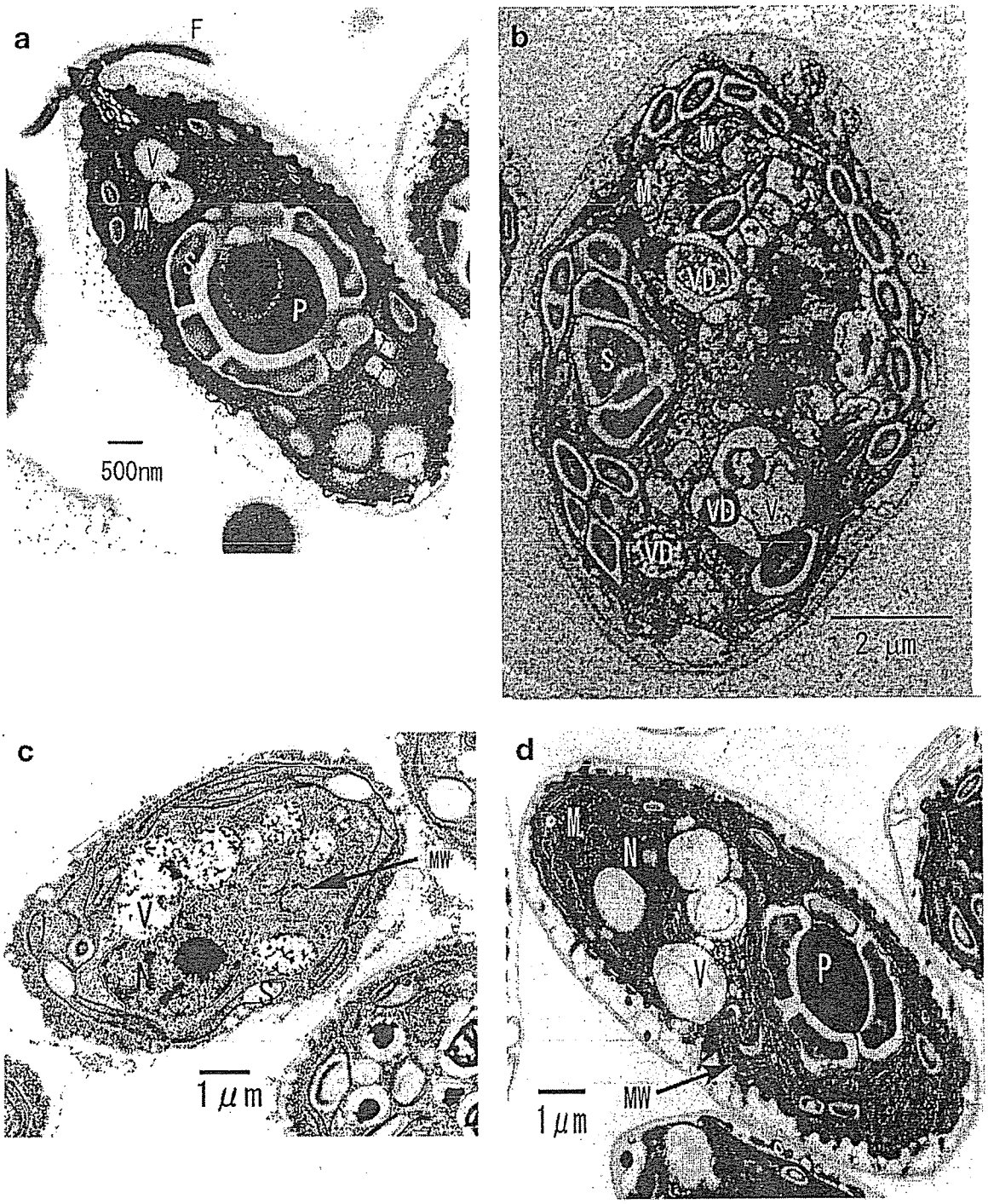

Fig. 1. Electron micrographs of *C. acidophila*. a: Untreated cell. b: Cell treated with 20 μM Cd for 3 days. Numerous starch granules (S) and vacuoles (V) were observed. c: Cell treated with 200 μm Cu. d: Cell treated with 1.5 mM Zn for 3 days. Abbreviations: F, flagella; M, mitochondria; MW, membrane whorl; N, nucleus; P, pyrenoid; S, starch granule; V, vacuole; VD, vacuolar deposit.

Table 1
Summary of morphometric analysis (mean values ± S.E.) in *C. acidophila* cells treated with metals for 3 days

	Treatments			
	Cellular area (μm^2)			
	Control	20 μM Cd	200 μM Cu	1.5 mM Zn
Whole cell	43.8 ± 3.82	59.7 ± 7.53*	27.4 ± 4.60*	37.0 ± 4.30
Cytoplasm	32.6 ± 3.59	47.8 ± 6.29*	22.9 ± 4.35	29.6 ± 4.07
Chloroplast	27.9 ± 3.26	46.3 ± 6.18**	22.0 ± 4.42	27.2 ± 3.80
Vacuole	10.5 ± 3.37	20.1 ± 4.0*	6.85 ± 2.81	8.12 ± 2.78
Starch	17.1 ± 2.39	41.6 ± 5.82**	9.56 ± 3.65	18.0 ± 2.74
Pyrenoid	2.22 ± 0.26	1.02 ± 0.10	1.69 ± 0.38	2.04 ± 0.26
Nucleus	3.45 ± 0.43	5.72 ± 0.92	3.58 ± 0.33	3.30 ± 0.26
Mitochondria	9.71 ± 2.99	9.41 ± 3.77	4.17 ± 1.62	1.79 ± 0.65

Over 20 microphotographs, each representing a separate cell, were scanned (Epson GT-7200U) and analyzed (NIH image program) to determine the organelle areas for each of the test conditions.
Statistically significant at: $*P < 0.05$, $**P < 0.01$ as calculated by one-way ANOVA.

The sizes of starch granules, vacuoles and chloroplasts were increased 2.43-fold ($P < 0.01$), 1.91-fold ($P < 0.05$) and 1.66-fold ($P < 0.01$), respectively. Conversely, pyrenoid structures were noticeably reduced in size to 46% of that of the controls. In addition, a new structure was formed after Cd treatment, consisting of non-membranous, electron-dense deposits, observed in vacuoles. This vacuolar deposit was of undefined shape and often occupied almost the whole vacuole (Fig. 1b). Vacuolar deposits were also observed in Cu- and Zn-treated cells (Fig. 1c,d).

All organelles decreased in size in Cu-treated cells. Although the size of the whole cell in Zn-treated cells decreased to 85% of that of the control cells, the size of starch grains of Zn-treated cells increased slightly. The presence of membrane whorls (MW) was observed in the Cu- and Zn-treated cells (Fig. 1c,d).

3.2. Accumulation of Cd

The presence of Cd clearly caused drastic ultrastructural changes (Fig. 1b). Cd accumulation within cells increased with time and the concentration was the highest in cells treated with 20 μM Cd for 3 days (Fig. 2). Cells were washed with EDTA before analysis and the obtained values represented intracellular Cd accumulations.

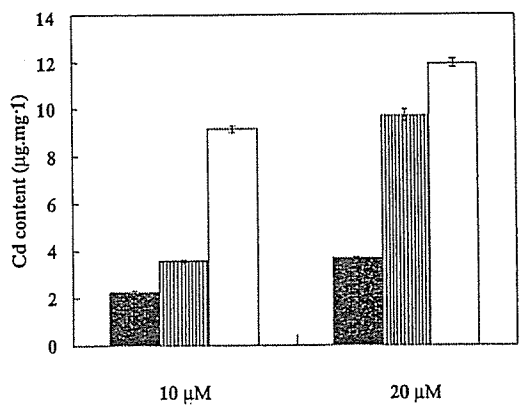

Fig. 2. Accumulation of Cd in *C. acidophila*. Accumulations of Cd after 10 and 20 μM Cd treatment for 1 day (dark gray bar), 2 days (striped bar), and 3 days (white bar).

3.3. Localization of Cd

X-ray microanalysis was performed to evaluate the local elemental distribution within the cell. The electron probe was focused on several analytical points including electron-dense deposits in vacuoles. An arrow in Fig. 3a shows one of the analytical points. In the EDX spectrum, signals of Cd and phosphate are clearly observed (Fig. 3b). Other signals represent Cu from the grid and Pb from the stain solution. Cd was also detected in the cell membrane. We confirmed that these electron-dense deposits contained both phosphate and Cd.

3.4. Effect of Cd on polyphosphate metabolism

Fig. 4 shows the effect of Cd stress on polyphosphate metabolism in *C. acidophila* as revealed by ^{31}P-NMR. After Cd treatment for 3 days, changes in the intensity of the polyphosphate peak and the vacuolar phosphate peak were apparent. The polyphosphate peak disappeared almost completely, accompanied by an intense increase in the vacuolar phosphate peak (Fig. 4a), suggesting that the two processes were related. To determine whether the disappearance of polyphosphate is reversible or not, Cd-treated cells were re-incubated in modified Sager–Granick medium for 3 days, and a ^{31}P-NMR spectrum was taken. Fig. 4c shows that the polyphosphate peak recovered to the previous level. In addition, a decrease in the vacuolar phosphate peak and the sugar phosphate peak increased. The phosphate level in the recovered cells did not return to the original level.

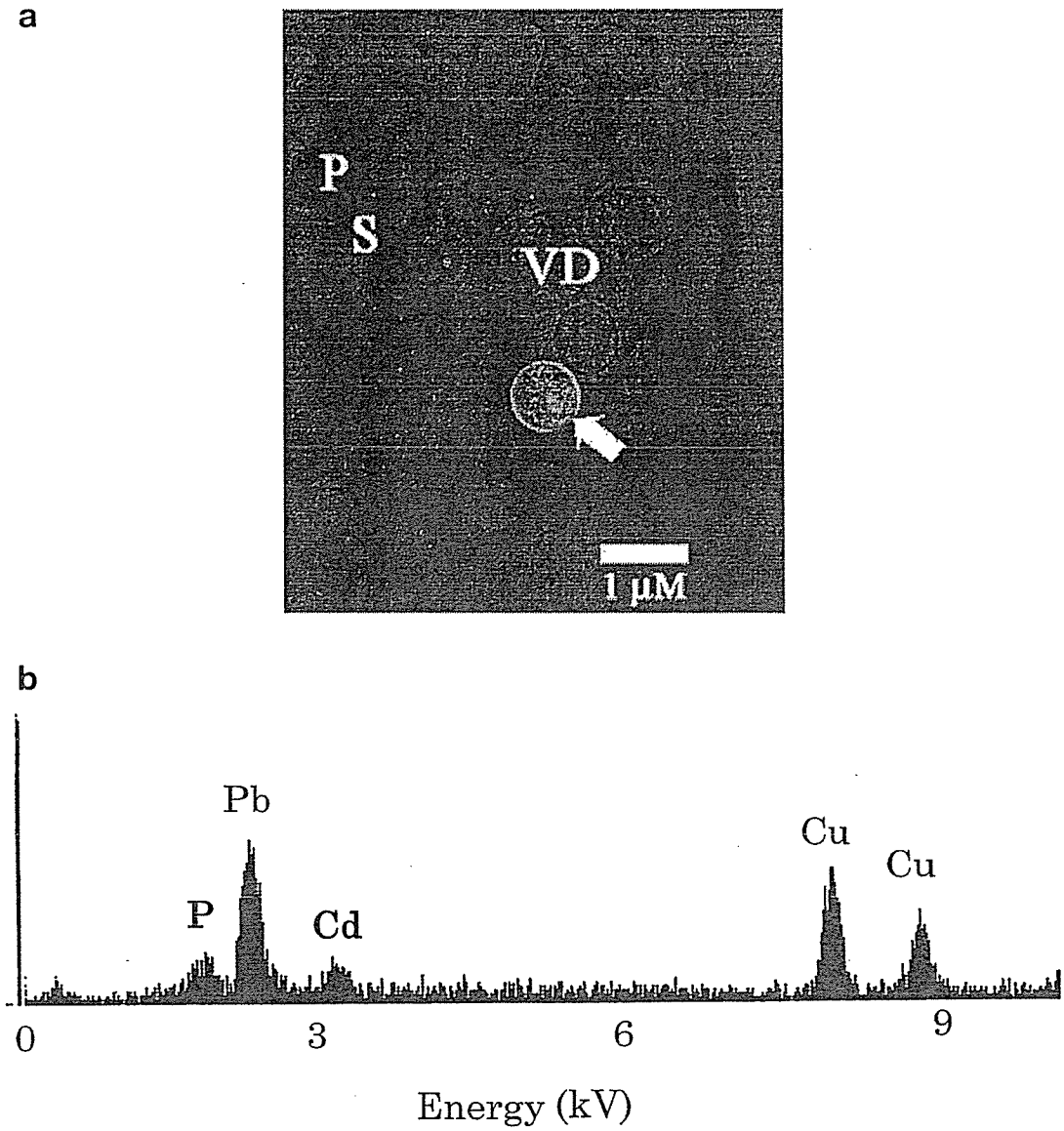

Fig. 3. The vacuolar deposits as determined by EDX analysis. a: Electron micrograph of *C. acidophila*. The arrow represents the region analyzed by EDX analysis. b: Spectra of vacuolar deposits in *C. acidophila* treated with 20 μM Cd for 3 days by EDX analysis.

4. Discussion

The three studied metals influenced *C. acidophila* cells differently, with the greatest ultrastructural change caused by cadmium. Although EC_{50} is one index for biological toxicity, it cannot reveal the exact cytological toxicity. Morphometric analysis at the ultrastructural level may provide ecologically valuable insights. This change involved enlargements of starch granules and vacuoles, a reduction in pyrenoid and mitochondrial size (Table 1) and the presence of MW and vacuolar deposits (Fig. 1b–d).

Similar increases in the starch granule size and a reduction in mitochondrial size were reported in *Chlorella* cells, in which the rapid deterioration of mitochondria caused accumulation of starch grains [13]. Mitochondria are a primary target of the cadmium-associated cytotoxicity in freshwater green algae [14]. Consequently, since the respiratory activities cannot be carried out without mitochondria, starch accumulation results in the disarrangement of the chloroplasts.

Rachlin et al. [7] detected accumulation of metals (Ni, Cu, Co, Zn, Cd, and Hg) in MW in *Plectonema boryanum* and suggested that this new structure was detached from residues of thylakoids for a cellular detoxification mechanism.

Enlargement of vacuoles and deposits inside the cells were the most remarkable changes but the shape of the deposits was difficult to define clearly. *C. acidophila* accumulated a large amount of Cd within cells (Fig. 2) and